

Return Loss Improvement of Radial Line Slot Array Antennas on Closed Ring Resonator Structure at 28 GHz

Abstract. This paper aims to investigate and design a radial line slot array antenna (RSLA) with closed ring resonator (CRR) for return loss improvement. The CRR printed on a dielectric substrate with a circumference alignment position attached to the RLSA antenna. The CRR structure used the combination of the four rings with a rectangular shape and showed a response in the range of 25.30 GHz up to 31.40 GHz. It is worth mentioning that applying a gap cavity height (h) of the superstrate layer to the CRR structure is needed to improve the return loss significantly. However, as the superstrate layer of the CRR structure is increased the value of the gap cavity height must be adjustable to ensure that the return loss is maintained at the same resonant frequency. The return loss performance showed a significant improvement from -10.30 dB to -12.34 dB for $\lambda/4$ gap between the antenna and the superstrate.

Streszczenie. Artykuł ma na celu zbadanie i zaprojektowanie radialnej anteny liniowej z matrycą szczelinową (RSLA) z rezonatorem zamkniętym pierścieniem (CRR) w celu poprawy strat odbiciowych. CRR wydrukowany na podłożu dielektrycznym z pozycją wyrównania obwodu przymocowaną do anteny RLSA. Konstrukcja CRR wykorzystywała kombinację czterech pierścieni o prostokątnym kształcie i wykazywała odpowiedź w zakresie od 25,30 GHz do 31,40 GHz. Warto wspomnieć, że zastosowanie wysokości wnęki szczelinowej (h) warstwy superstratu do struktury CRR jest potrzebne do znacznej poprawy strat powrotnych. (Poprawa tłumienia odbicia anten radialnych z matrycą liniową w strukturze rezonatora z zamkniętym pierścieniem przy 28 GHz)

Keywords: Radial Line Slot Array (RSLA), Ka-band, Millimeter-Wave, Air Gap RSLA, Closed Ring Resonator (CRR), RT Duroid 5880

Słowa kluczowe: antena radialna, tłumienie odbicia, rezonator

Introduction

The design of the radial line slot array (RLSA) antenna is already saturated nowadays, for example, many techniques of slots arrangement of the radiating plates had been applied such as spider RLSA [1] beam squint [2], [3] and reflection cancelling slot [4], [5] RLSA antenna. However, most researchers move to do the research using a substrate FR4 board to RT Duroid 5880 based on high-frequency ranges for Millimeter-Wave application.

The RLSA antennas were recently found a complicated compact size such as the honeycomb structures [6]–[8]. The low profile makes this kind of antennas used for Nomex® paper and Quartz fabric as a dielectric medium. Moreover, their frequencies were used for 32 GHz and provided a high gain characteristic. Furthermore, there are two waves that the RLSA provided, such as standing and inward travelling waves by enforcing both cylindrical aperture distributions of RLSA [9]–[13]. The frequencies have been through the research is on 62.5 GHz [9], 12 GHz [10] and 15 GHz [11]–[13]. Hopkins mentioned the frequencies of 7.2 GHz and 8.4 GHz is designed for X-band Deep Space Network (DSN) by applying circular waveguide [14]. However, using the metamaterial on the RLSA antenna is another way to enhance the antenna parameter. There are few metamaterial structures proposed to improve the antenna performance such as frequency selective surface (FSS) [15], [16], split ring resonator (SRR) [17], [18] and electromagnetic band-gap (EBG) [19]–[21]. However, there is no antenna made with metamaterial on RLSA structure. Moreover, the proposed antenna is evaluated based on the effectiveness of the design and will be compared with the conventional RLSA antenna. The selected frequency is at 28 GHz, which is in the range of Ka-band. A few techniques and designs to enhance the bandwidth and gain for 5G and millimetre-wave applications are also presented [22]–[24].

This paper proposes a new technique on the RLSA antenna structure with a circular ring resonator (CRR) structure. The enhancement of return loss for RLSA antenna with a single superstrate layer as the resonant frequency of 28 GHz is

introduced. The two values of height, h are proposed, which are $\lambda/2$ and $\lambda/4$, respectively. The antenna achieves a simulated return loss of -12.34 dB for -12.34 dB and -10.30 dB for $\lambda/4$ significantly in linear polarization.

RSLA antenna design

To develop the RLSA array antenna, the simulation via the software CST microwave produced the rectangular slot length shaped with the diameter of the antenna's radiating surface of about 100 mm, as shown in Fig.1. By referring the parameters represented in Table 1, the calculated value for the rectangular slot length is $\lambda/2 = 5$ mm, and the width found to be 1 mm. The position of the feeder port is located at the back, and the pin of SSMA 50 Ohms is touched in the middle between the two slots in the centre of radiating plate. The numbers of slots in the first ring are 16.

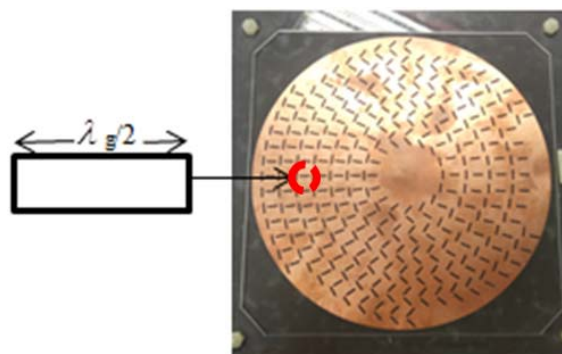


Fig.1. Structure of conventional RLSA antenna and the radiating shape

The antenna is designed to operate at 28 GHz. For this design, the Roger RT 5880 substrate was used for the fabrication process comes with a dielectric material of ($\epsilon_r = 2.2$), and dielectric loss tangent ($\tan \delta$) of 0.0009. The height of the substrate (h) was 0.254. The SSMA connector was used which is considered as a miniature version of

SMA connector. A coaxial probe attaches the radial line slot array antenna, the coaxial probe of 50 Ω and the feed point is located in the middle between the rectangular slots on the radiating plate where the feed pin passes through the cavity thickness which means the ground plane and air gap are touching the substrates.

Table1. Design specification of RLSA antenna

Parameters	Values (mm)
Radius of antenna	50
Cavity of thickness (Minimum)	2.254
Thickness of radiating surface (copper)	0.035
Thickness of ground (copper)	0.035
Slot width	1.0
Slot length	5.0

The cavity structure consists of hybrid RT5880 and air gap. The substrate and air gap structures are calculated to be a single substrate. The air has 1.0 values of dielectric constant as duplicated in Fig. 2.

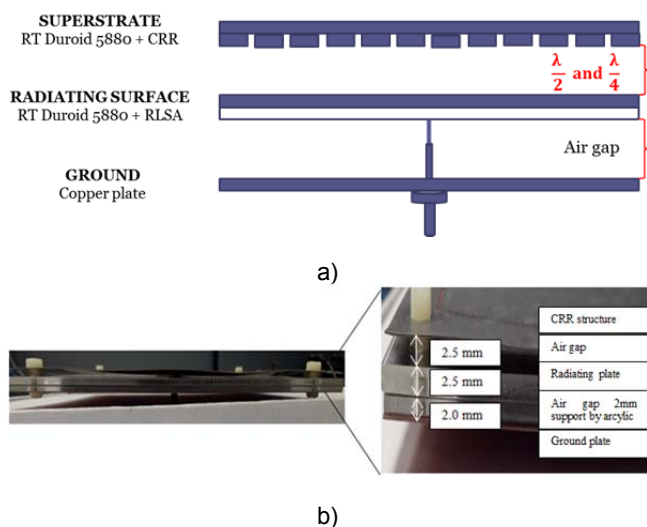


Fig.2. The open-ended air gap structure RLSA antenna on RT Duroid 5880 by side view in both a) Two-dimensions and, b) Three dimensions for $\lambda/2$ and $\lambda/4$

CRR design structure

The metamaterial design, antennas, microwave absorbers, mixers, filters, and oscillators use a split ring resonator (SRR) design in microwave application. The SRR has the potential to raise the reflection loss or S11 results of the microwave absorber [25]. There are few types of the split-ring resonator that quite familiar in antenna and RF researchers which are edge couple split ring resonator (EC-SRR), Broadside couple split ring resonator (BC-SRR), non-bianisotropic couple split ring resonator (NC-SRR), spiral resonator and many others. To miniaturization of the resonant particles is the main objective of the split ring resonator structures. The split ring resonator can reduce the electric size by increasing the coupling effect between the individual rings of the split ring resonator. The contraction of the electrical size in the split ring resonators can raise the coupling effect between the individual rings.

There may exist the coupling effect between the two circular rings, as presented in Fig. 3. Where the proposed structures consisting of printed resonating elements on two surfaces which top and bottom and, in the middle, attached with a full copper layer to achieve dual resonance. The equation for the simulated structure had been applied as below:

$$(1) \quad r = \frac{\lambda_{go}}{2\pi} = \frac{\lambda_o}{2\pi\sqrt{\epsilon_{re}}} = \frac{300}{2\pi f_o(GHz)\sqrt{\epsilon_{re}}}$$

$$(2) \quad \epsilon_{re} = \frac{\epsilon_r + 1}{2} + \frac{\epsilon_r - 1}{2} \left(\left(1 + 12 \frac{h}{w_r}\right)^{0.5} + 0.04 \left(1 - \frac{w_r}{h}\right)^2 \right)$$

$$(3) \quad f_o = \frac{300}{\pi(r_o + r_i)\sqrt{\epsilon_{re}}}$$

where: r – radius of a circular ring, r_o – outer radius of a circular ring, r_i – inner radius of a circular ring, λ_{go} – guided wavelength at resonance, ϵ_{re} – effective relative resonance frequencies

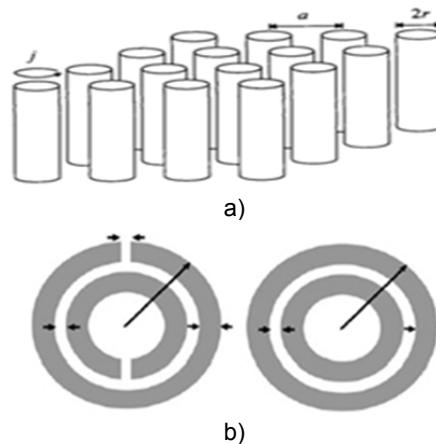


Fig.3. a) an array structure of metallic split-ring resonator. b) design for split-ring resonator (SRR) on the right and left is the closed ring resonator (CRR)

Fig. 4 and Table. 2 shows the CRR structure designed to be used in this research and the parameter values for a unit cell of CRR structure. These CRR structures must be placed at the superstrate layer's circumference located at the above layer of the RLSA antenna.

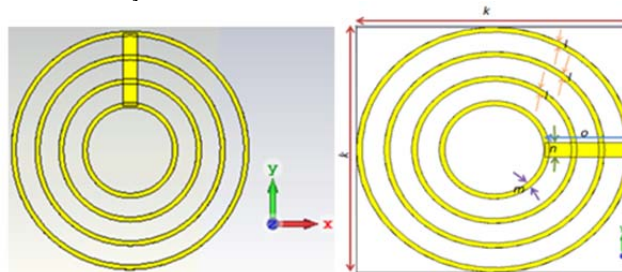


Fig. 4. The design of a unit cell CRR structure

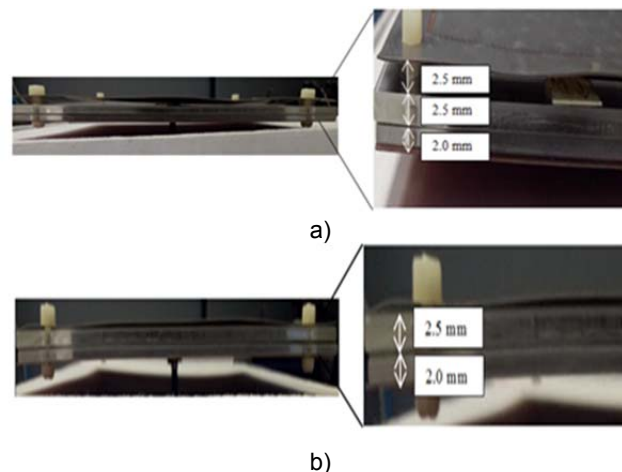


Fig. 5. Fabricated superstrate above the air gap of RLSA antenna in both sizes a) 5mm and, b) 2.5mm

Table. 2 The following dimension value for the unit cell CRR structure design

Alphabet for a unit cell CRR	Optimization range (mm)
<i>k</i>	5.0
<i>l</i>	0.05
<i>m</i>	0.1
<i>n</i>	0.15
<i>o</i>	0.7925

The gap cavity height, *h* is increased by 2.5 mm shows is shown in Fig. 5. Simultaneously as presented in [26]. Wang stated by applying and adjusting the height resonator, which is known as gap cavity height and the size of the FSS to enhance the gain because the electromagnetic wave can continuously reflect the cavity.

Results and discussion

There are three proposed design RLSA antenna have been simulated such as conventional, RT Duroid 5880 at $\lambda/2$ and RT Duroid at $\lambda/4$ of the gap cavity height of superstrate layer CRRs has well explained. The parametric study has been carried out for the separation or also known as a gap of the one layer of the circumference CRR structure. Two comparisons have been made for the distance of $\lambda/2$, which equivalent to 5 mm and decrement to $\lambda/4$, which equal to 2.5 mm away from the original RLSA antenna as presented in Fig. 5.

The closed ring resonator structure can only work at a single frequency of 28 GHz, as shown in Fig. 6. The reflection coefficient of one element of CRR produced S11 results more than -40 dB and have a wider bandwidth from 25.38 GHz to 31.38 GHz which around 6 GHz. Besides, the simulated result of the proposed 28 GHz reconfigurable in the band-stop state.

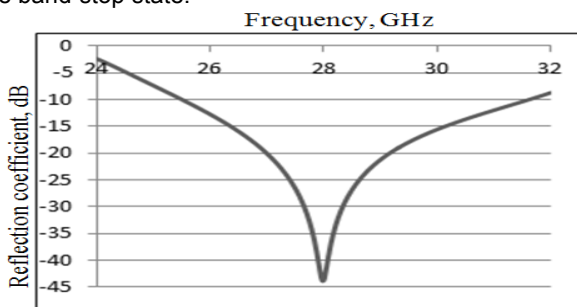


Fig. 6. Simulated return loss result of CRR structure

The simulated and measured reflection coefficient (S11) results are presented in Fig. 7 and Fig. 8. The return loss for RLSA without CRR with blue colour at 28 GHz is -11.42 dB. The highest resonance at 25.23 GHz showed a return loss of 22.06 dB. The graph exhibits the bandwidth started from 26.92 GHz to 28.14 GHz frequency, and the response is below than -10 dB for return loss. Meanwhile, the $\lambda/2$ is equivalent to 5 mm as the green colour shows the return loss at 28 GHz is -12.34 dB. Therefore, the strongest resonant for simulated is at 25.40 GHz with a return loss performance of -22.24 dB and for the measured results is at 25.53 GHz with -29.03 dB of return loss performance. The bandwidth started from 24.88 GHz frequency, and the response is below than -10 dB of return loss continues until 28.34 GHz for simulated results. The frequency range from 27.53 GHz to 28.34 GHz gave a bandwidth of 0.81 GHz. The bandwidth specified by the ITU is from 27.5 to 28.35 GHz, it is the range of downlink band. Therefore, the simulated and measures return loss showed the response has covered the required bandwidth and covered a millimetre-wave at 28 GHz. The $\lambda/4$ is the red colour indicates the return loss at 28 GHz and -10.24 dB for return loss value. The strongest resonant for simulated is at 25.18 GHz with a return loss reported at -23.54 dB and 25.53 GHz

for the measured results with -25 dB return loss performance. The bandwidth started from 24.78 GHz frequency, and the response is below than -10 dB of return loss continues until 28 GHz for measuring results. The frequency from 27.17 GHz to 28.03 GHz indicates that the 28 GHz of bandwidth range is included. The bandwidth specified by the ITU is from 27.5 to 28.35 GHz, it is the range of downlink band. Therefore, the simulation and measurement return loss showed the response had covered the required bandwidth.

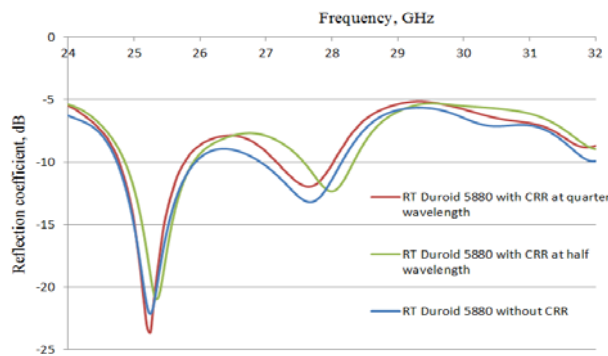


Fig. 7. Comparison of the reflection coefficient (dB) versus frequency (GHz) of simulation results

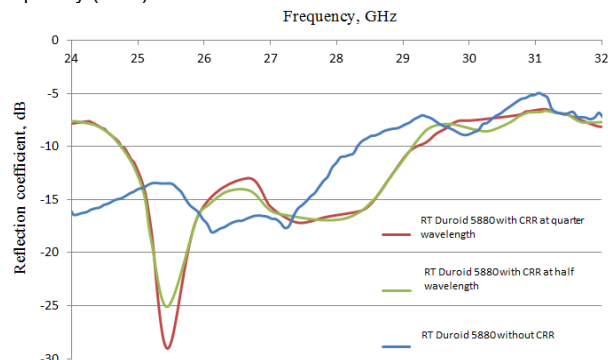


Fig. 8. Comparison of the reflection coefficient (dB) versus frequency (GHz) of measurement results

The effect of increasing the cavity height, "h" of the superstrate layer of the CRR structure is proposed. The results in a considerable increase in the return loss because of the combination of the hybrid Air gap RLSA antenna with a superstrate layer of CRR structure. There is a minor shift in frequency to the right and exactly falls on 28 GHz for the RT 5880 at 2.5 mm. However, the RT 5880 at 5 mm is exactly resonant at 28 GHz of the centre frequency range. The comparison results between the simulated and measured results are listed in Table. 3.

Table. 3 The performance cavity height of the superstrate layer of RLSA antenna

Antenna	Simulation	Measurement
RT Duroid 5880 without CRR	-11.42	-11.01
RT Duroid 5880 with CRR at quarter wavelength	-12.34	-15.04
RT Duroid 5880 with CRR at half-wavelength	-10.24	-17.19

The radiation pattern for both models is simulated for the high characteristic performance of millimetre-wave air gap RLSA. The radiation patterns are presented in the Cartesian plane, as shown in Fig. 9. The RT Duroid 5880 with CRR at $\lambda/2$ performed a high gain of 20.02 dB, and 20.41 dBi of directivity. Meanwhile, the RT Duroid 5880 with CRR at $\lambda/4$ offered a peak gain of 19.43 dB with 20 dBi of total directivity.

Next, for $\lambda/2$, the sidelobe level (SLL) is about -10.70 dB at the E plane while the SLL for H plane is -2.80 dB. This antenna also provides a 38.28 dB front to the back-lobe ratio at E and H plane. Hence, the main lobe is squinted 18° to the left. The $\lambda/2$ with air gap RLSA has a half-power beamwidth (HPBW) of 7.10 degree and 22.0 degree in E and H planes, respectively. Then, for $\lambda/4$ the -18.46 dB sidelobe level is recorded at the E plane while H plane value is at -9.10 dB. This antenna also provides 36.25 dB front to the back-lobe ratio at E and H plane. Hence, the main lobe squinted 2° to the left. The $\lambda/4$ with air gap RLSA has a half-power beamwidth (HPBW) of 7.70 and 21.60 degrees in the E and H planes.

The comparison between the simulation and measurement results for E-plane and H-plane are tabulated in Table. 4. The gain value of the measurement result slightly differs from the simulated result. It is due to the losses from the cable, which is -3 dB. The measured value shows a good agreement with the simulated results because both sidelobe level (SLL), and back lobe level (BLL) is below than -10 dB and -20 dB, without CRR structure.

The gain value slightly differs to 0.270 dBi for the simulated result. The measured H-plane received more than 20 dB for the back-lobe value of ripple, because of the cable dislocated from the slot, and may due to the circumference of CRR structure does not mesh with the RLSA antenna with CRR structure at $\lambda/4$ distance.

The simulation and measurement radiation pattern of RT Duroid 5880 with air gap RLSA at 28 GHz without CRR, and with CRR at $\lambda/2$ and CRR at $\lambda/4$ with air gap RLSA at 28 GHz are registered in Table 4. The measured result for gain slightly differs from the simulated due to the

fabrication's effect, and more about the material used to contact the ground plane with the SMA port, which is screwed. The 3D views show an advantage in a point-to-point communication system.

Table 4. The summary of simulation and measurement radiation pattern of RT Duroid 5880 with air gap RLSA at 28 GHz without CRR, with CRR at $\lambda/2$ and CRR at $\lambda/4$ with Air Gap RLSA at 28 GHz.

Antenna Parameter	Simulation			Measurement		
	Without CRR	With CRR	With CRR	With out CRR	With CRR	With CRR
		$\lambda/2$	$\lambda/4$		$\lambda/2$	$\lambda/4$
Gain (dBi)	19.750	20.020	19.430	19.091	19.480	19.700
Beamwidth at -3 dB	8.700 5.900	7.100 22.000	7.700 0	7.200 0	9.000 0	1.800 6.600
>E plane (degree)		0	21.600	2.567	1.800	0
>H plane (degree)						
Main to Side Lobe Ratio (dB)	21.920 9.508	22.360 5.600	18.460 9.100	18.777 25.200	16.449 17.281	48.600 24.750
>E plane						
>H plane						
Front to Back Ratio (dB)	42.469 21.783	42.760 19.080	36.586 22.546	27.478 33.800	26.246 26.632	22.562 12.650
>E plane						
>H plane						

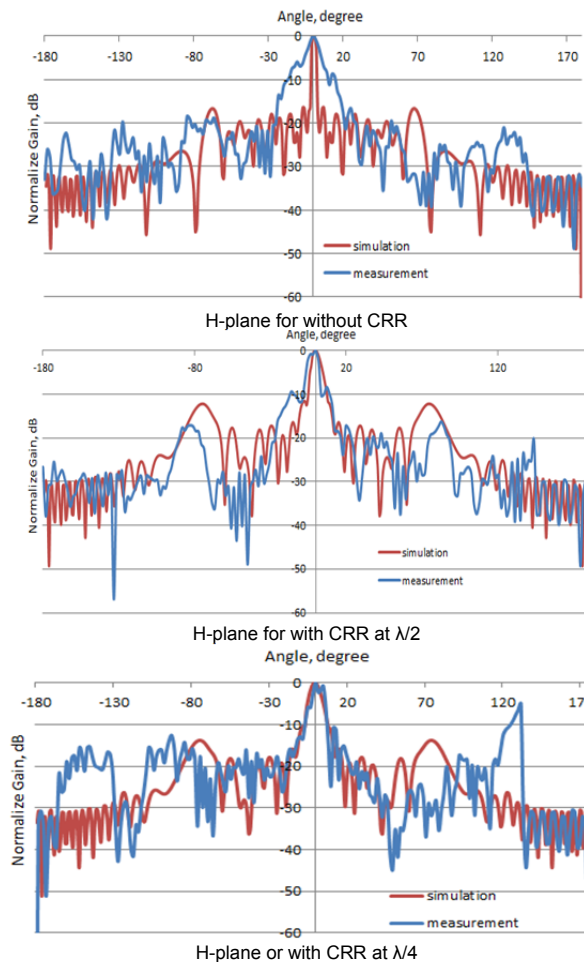
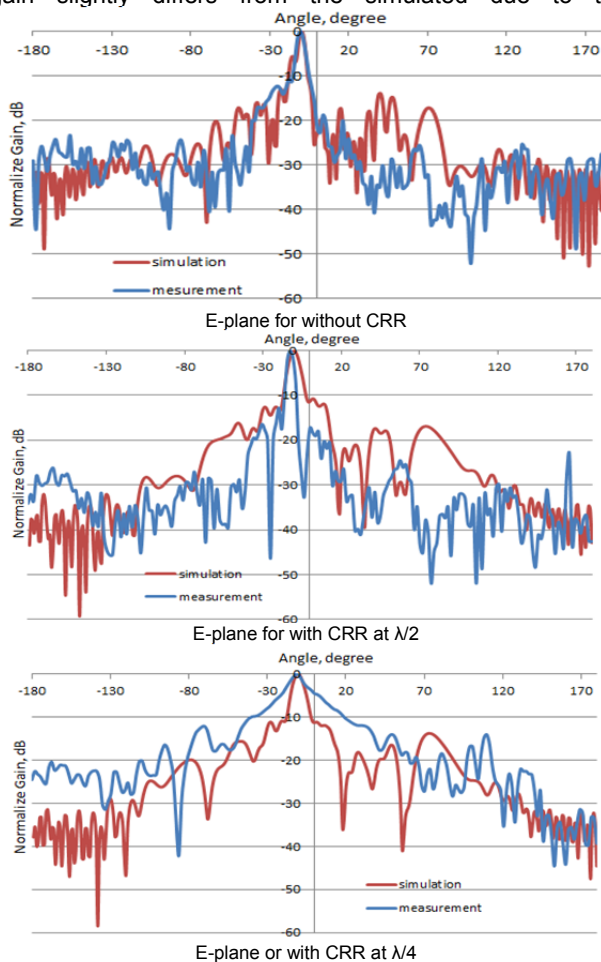


Fig. 9. Simulated and measured for E-plane and H-plane results between RT Duroid 5880 without CRR, RT Duroid 5880 with CRR at the distance of $\lambda/4$ and $\lambda/2$

Conclusion:

As discussed, the CRR structure suppresses the surface wave propagation. The improvement of return loss with high gain is obtained. The air gap of cavity height, "h" is adaptive. The gap of cavity height of $\lambda/2$, which is 5 mm shifted to the right due to inductive, L and resonate frequency at the centre of 28 GHz. This kind of antenna is working on millimetre wave as an effective way for a 5G communication and point to point system.

Authors: The first five authors are came from the same university and faculty, which is Universiti Teknikal Malaysia Melaka (UTeM), Jalan Hang Tuah Jaya, 76100 Durian Tunggal, Melaka, Faculty of Electronics and Computer Engineering. Their emails are as follows:

rabiataluzian93@gmail.com.my, imranibrahim@utem.edu.my, engah med_jamall@yahoo.com, zahriladha@utem.edu.my, noorazwan@utem.edu.my. T.A. Rahman from Universiti Teknologi Malaysia (UTM), School of Electrical Engineering, Sultan Ibrahim Chancellery Building, Jalan Iman, 81310 Skudai, Joho. tharek@fke.utm.my. T. Purnamirza from Sultan Syarif Kasim II State Islamic University, Jalan HR. Soebrantas Panam Km. 15 No. 155, Tuah Madani, Kec. Tampan, Kabupaten Kampar, Riau 28293, Indonesia, tptambusai@yahoo.com.

REFERENCES

- [1] W. A. W. Muhamad, T. A. Rahman, and M. F. Jamlos, "The Effects of Air-Gap on Spider Radial Line Slot Array (SRLSA) Antenna for Point to Point Application," in *2013 IEEE Symposium on Wireless Technology & Applications (ISWTA)*, 2013, pp. 388–390.
- [2] M. I. Imran, A. Riduan, A. R. Tharek, and A. Hasnain, "Beam Squinted Radial Line Slot Array Antenna (RLSA) Design for Point- to-Point WLAN Application," in *2007 Asia-Pacific Conference on Applied Electromagnetics*, 2007.
- [3] M. I. Imran, A. R. Tharek, and A. Hasnain, "An Optimization of Beam Squinted Radial Line Slot Array Antenna Design at 5 . 8 GHz," in *2008 IEEE International RF and Microwave Conference*, 2008, pp. 139–142.
- [4] P.W.Davis and M.E.Bialkowski, "Comparing Beam Squinting and Reflection Cancelling Slot Methods for Return Loss Improvement in RLSA Antennas," in *IEEE Antennas and Propagation Society International Symposium 1997. Digest*, 1997, pp. 1938–1941.
- [5] T. S. Lim, A. R. Tharek, W. A. W. Khaimddin, and A. Hasnain, "Prototypes Development for Reflection Canceling Slot Design of Radial Line Slot Array (RLSA) Antenna for Direct Broadcast Satellite Reception," in *Asia-Pacific Conference on Applied Electromagnetics, 2003. APACE 2003.*, 2003, pp. 34–37.
- [6] T. Nguyen, J. Hirakawa, M. Anda, O. Amana, S. Kareeda, and T. Matsuzaki, "Material Choices of Honeycomb Structures and their Effects in mm-Wave RLSAs," in *2014 IEEE Fifth International Conference on Communications and Electronics (ICCE)*, 2014, pp. 417–419.
- [7] T. Nguyen *et al.*, "Study of Material Loss in mm-Wave RLSA with Honeycomb Structure," in *2013 IEEE Antennas and Propagation Society International Symposium (APSURSI)*, 2013, pp. 328–329.
- [8] T. Nguyen *et al.*, "A Concise Design of Large mm-Wave Radial Line Slot Antenna with Honeycomb Structures for Space Application," in *2014 XXXIth URSI General Assembly and Scientific Symposium (URSI GASS)*, 2014.
- [9] S. C. Pavone, A. Mazzino, A. Freni, and M. Albani, "Wideband analysis of RLSA Bessel beam launchers based on standing and inward traveling wave aperture distributions for electromagnetic pulse generation," in *2017 11th European Conference on Antennas and Propagation (EUCAP)*, 2017, pp. 3649–3652.
- [10] M. Ettore *et al.*, "Experimental Validation of Bessel Beam Generation Using an Inward Hankel Aperture Distribution," *IEEE Trans. Antennas Propag.*, vol. 63, no. 6, pp. 2539–2544, 2015.
- [11] A. Mazzino *et al.*, "Bessel Beam Generation with a RLSA Antenna for Non-Contact Detection of Buried Objects," in *The 8th European Conference on Antennas and Propagation (EuCAP 2014)*, 2014, pp. 762–766.
- [12] A. Mazzino *et al.*, "Large Depth of Field Pseudo-Bessel Beam Generation With a RLSA Antenna," *IEEE Trans. Antennas Propag.*, vol. 62, no. 8, pp. 3911–3919, 2014.
- [13] A. Mazzino *et al.*, "Bessel Beam Generation with a RLSA Antenna," in *ICECom 2013*, 2013, pp. 3–6.
- [14] M. Bray and J. H. Road, "A Radial Line Slot Array Antenna for Deep Space Missions," in *2017 IEEE Aerospace Conference*, 2017.
- [15] A. J. A. Al-gburi, I. M. Ibrahim, M. Y. Zeain, and Z. Zakaria, "Compact Size and High Gain of CPW-fed UWB Strawberry Artistic shaped Printed Monopole Antennas using FSS Single Layer Reflector," *IEEE Access*, vol. 8, no. 5, pp. 92697–92707, 2020.
- [16] A. J. A. Al-gburi *et al.*, "A compact UWB FSS single layer with stopband properties for shielding applications," *Przeegląd Elektrotechniczny*, no. 2, pp. 165–168, 2021.
- [17] A. J. A. Al-gburi, I. M. Ibrahim, and Z. Zakaria, "Band-notch effect of U-shaped split ring resonator structure at ultra wide-band monopole antenna Band-notch Effect of U-shaped Split Ring Resonator Structure at Ultra Wide-band Monopole Antenna," *Int. J. Appl. Eng. Res.*, vol. 12, no. 15, pp. 4782–4789, 2017.
- [18] I. M. Ibrahim, A. J. A. Al-gburi, Z. Zakaria, and H. A. Bakar, "Parametric Study of Modified U-shaped Split Ring Resonator Structure Dimension at Ultra-Wide-band Monopole Antenna," *J. Telecommun. Electron. Comput. Eng.*, vol. 10, no. 2–5, pp. 53–57, 2018.
- [19] A. J. A. Al-Gburi, I. Ibrahim, and Z. Zakaria, "Gain Enhancement for Whole Ultra-Wideband Frequencies of a Microstrip Patch Antenna," *J. Comput. Theor. Nanosci.*, vol. 17, no. 2–3, pp. 1469–1473, 2020.
- [20] A. J. Abdullah Al-Gburi, I. M. Ibrahim, Z. Zakaria, and A. D. Khaleel, "Gain Improvement and Bandwidth Extension of Ultra-Wide Band Micro-Strip Patch Antenna Using Electromagnetic Band Gap Slots and Superstrate Techniques," *J. Comput. Theor. Nanosci.*, vol. 17, no. 2–3, pp. 985–989, 2020.
- [21] A. J. A. Al-Gburi, I. Ibrahim, and Z. Zakaria, "A Miniature Raspberry Shaped UWB Monopole Antenna based on Microwave Imaging Scanning Technique for Kidney Stone Early Detection," *Int. J. Psychosoc. Rehabil.*, vol. 24, no. 2, pp. 1755–1763, 2020.
- [22] M. Y. Zeain *et al.*, "Design of helical antenna for next generation wireless communication," *Prz. Elektrotechniczny*, no. 11, pp. 96–99, 2020.
- [23] H. H. Keriee *et al.*, "High gain antenna at 915 mhz for off grid wireless networks," *Bull. Electr. Eng. Informatics*, vol. 9, no. 6, pp. 2449–2454, 2020.
- [24] M. Y. Zeain *et al.*, "Design of a wideband strip helical antenna for 5G applications," *Bull. Electr. Eng. Informatics*, vol. 9, no. 5, pp. 1958–1963, 2020.
- [25] H. Nornikman, B. H. Ahmad, M. Z. A. A. Aziz, F. Malek, H. Imran, and A. R. Othman, "Study and Simulation of An Edge Couple Split Ring Resonator (EC-SRR) on Truncated Pyramidal Microwave Absorber," *Prog. Electromagn. Res. PIER*, vol. 127, no. 3, pp. 319–334, 2012.
- [26] Y. Wang and D. Piao, "A High-Gain Resonant Cavity Antenna with Orthogonal Polarizations Working at 28 GHz," in *2016 IEEE 9th UK-Europe-China Workshop on Millimetre Waves and Terahertz Technologies (UCMMT)*, 2016, pp. 248–250.